ISSN 0036-0295, Russian Metallurgy (Metally), Vol. 2015, No. 4, pp. 278–284. © Pleiades Publishing, Ltd., 2015.
Original Russian Text © S.V. Ovchinnikov, A.D. Korotaev, Yu.P. Pinzhin, 2014, published in Deformatsiya i Razrushenie Materialov, 2014, No. 3, pp. 24–32.

PROMISING MATERIALS AND TECHNOLOGIES

Modification of the Microstructure of TiN-Based Columnar Coatings in Indentation Zones

S. V. Ovchinnikov[a, *], A. D. Korotaev[b], and Yu. P. Pinzhin[a]

[a] *Institute of Strength Physics and Materials Science, Siberian Branch, Russian Academy of Sciences, pr. Akademicheskii 2/4, Tomsk, 634021 Russia*

**e-mail: ovm@spti.tsu.ru*

[b] *Tomsk State University, Novosobornaya pl. 1, Tomsk, 634050 Russia*

Received September 18, 2013; in final form, November 19, 2013

Abstract—The columnar structure of titanium nitride–based coatings deposited by magnetron sputtering is studied. The structure–phase state of the coatings is analyzed after deposition and in the indentation zone. The type of dislocation structure, the grain size, the subgrain size, the misorientations at boundaries, and their change during coating growth are determined. The detected decrease (several tens of percent) in the coating thickness under an indenter indicates plastic deformation of a coating. On a microscopic level, this deformation manifests itself in an increase in the density, the misorientation, and the nonequilibrium of boundaries.

DOI: 10.1134/S0036029515040126

1. INTRODUCTION

According to the data of numerous studies (see, e.g., [1–5]), low-alloy titanium nitride–based coatings usually have submicrocrystalline grains elongated in the growth direction, i.e., a so-called columnar structure. The specific features of this structure implies competition of the growth of columnar grains with texture formation and depend on the growth activation energy (ion energy, temperature), the substrate orientation, the gas partial pressure, and some other factors [6–9]. Most results of these works are based on describing the macroscopic picture of coating growth obtained by scanning electron microscopy and X-ray diffraction [2, 3, 8, 9]. Therefore, some obtained dependences, such as the change in texture induced by a change in the deposition conditions [9], have no structural grounds.

Using transmission electron microscopy, the authors of [1, 4, 5, 10, 11] studied the structure of columnar coatings in the growth direction (in cross section), determined the column diameters in a columnar structure and the influence of a substrate of the column sizes (no division into grains or subgrains was performed in those works), and detected dislocations and low-angle boundaries. However, these data are incomplete and mainly qualitative. For example, dislocations were detected but characteristic dislocation structures and the dislocation density were not determined, and low-angle boundaries were detected but data on their density and misorientation at boundaries were not presented [10, 12, 13].

It is also known that titanium nitride–based columnar coatings have a relatively low fracture toughness, at most 10–15 MPa $m^{0.5}$ [14]. Therefore, the formation of various cracks, namely, radial, inclined, edge cracks, is the main deformation mechanism during the indentation of coatings on soft (steel) substrates [15–17]. The data on the modification of a defect structure in the indentation zone are scarce. In particular, only the authors of [17, 18] noted that individual high-angle boundaries form under the indenter tip. The mechanism of their formation and the related structure relaxation effects were not discussed in those works. The authors of [16–21] performed an electron-microscopic investigation of the indentation zones and found no action of dislocation deformation mechanisms on the dislocation density. In addition, the authors of [19] detected material extrusion at the periphery of an indentation and material bending in the indentation zone, which were caused by the generation of geometrically necessary dislocations, and observed stress relaxation in the zone of cross cracks via dislocation motion.

The purpose of this work is to obtain the quantitative characteristics of a microstructure by dark-field electron-microscopic analysis of a lattice orientation, which makes it possible to determine local spectra and characteristics of structural defects (dislocations, low-angle boundaries) [22, 23]. To localize deformation in a substrate, the hardness of the substrate material (T15K6 hard alloy) was chosen to be comparable with that of the coating.

2. EXPERIMENTAL

Ti–Al–Si–Cu–N coatings were deposited by reactive magnetron sputtering of targets made of titanium (VT1-0 alloy, sputtering power of 2.4 kW), $Al_{60}Si_{40}$ alloy (sputtering power of 0.2 kW), and commercial-purity copper (sputtering power of 0.1 kW) in argon and nitrogen atmosphere using two assisted sources of gas (nitrogen) plasma onto substrates made of T15K6 ((in wt %) 79WC, 15 TiC, 6 Co) and subjected to planetary rotation. A coating was deposited at a pulsed bias voltage of –200 V and a substrate temperature of ≈150°C for 120 min, and the nitriding of a titanium sublayer was performed at a negative bias voltage of 6 kV applied to a substrate. The coating thickness along with the sublayer was about 0.85 μm.

The elemental composition of the coatings was determined by energy dispersive electron-probe microanalysis using the Genesis Software Version 5.1 software package. The nanohardness of the coatings was carried out using the TTX NHT^2 (CSM) system in the load range up to 350 mN, and load–indentation depth curves were recorded. Structural studies were performed with scanning (SEM-515, Philips) and transmission (CM-12, Philips) electron microscopes.

3. RESULTS AND DISCUSSION

3.1. Micro- and Substructure of the Deposited Coatings

Under the chosen deposition conditions, the coating has the following composition (at %): 49.0 Ti, 2.1 Al, 0.1 Si, 2.7 Cu, and 46.1 N. Note that the total concentration of alloying elements, in particular, silicon (which favors grain refinement [24]), is low (less than 5 at %). Therefore, we expected the formation of a coating structure with relatively large grains, which was supported experimentally.

The identification of electron diffraction patterns points to the formation of a single-phase B1 structure of alloyed TiN with lattice parameters $a = 0.422 \pm 0.001$ and 0.418 ± 0.001 nm in the coating plane and in the cross section, respectively (Fig. 1). The electron diffraction pattern taken from the cross section also contains reflections of α-Ti, which is obviously the part of the α-Ti sublayer that has not reacted with nitrogen upon nitriding.

The electron diffraction pattern taken from a region about 1 μm in size in the coating plane demonstrates an in-plane {110} texture and wide (up to 40°) azimuthal misorientations (Fig. 1a). The electron diffraction pattern taken from the cross section indicates the presence of several crystals of different orientations (Fig. 1b), which can correspond to a {110} texture in the presence of the mechanism of competitive growth of columnar grains (which is well known for columnar coatings). The operation of this mechanism can be supported by dark-field electron-microscopic analysis of the bending–torsion of a crystal lattice in the sections that are parallel to the coating growth direction [22, 23].

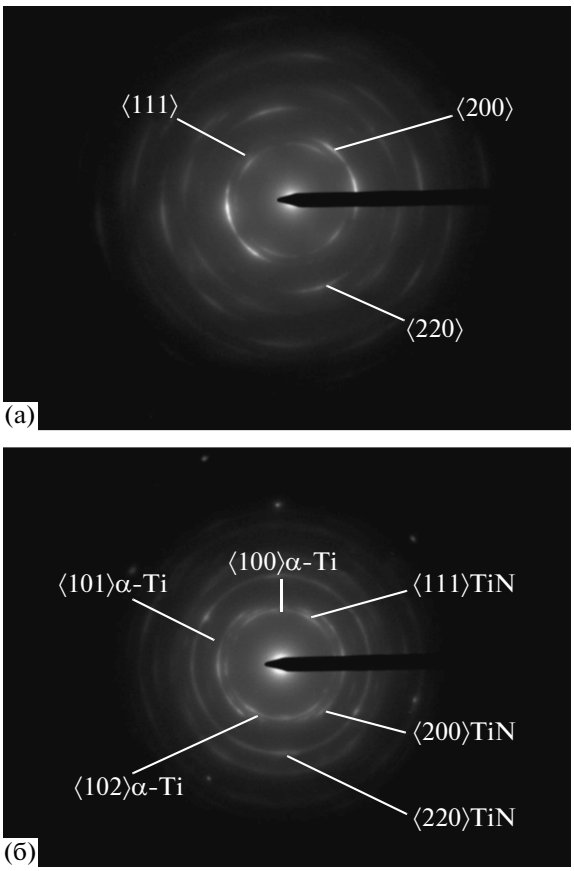

Fig. 1. Electron diffraction patterns taken from (a) surface layer and (b) cross section of a titanium nitride–based coating.

Figure 2 shows fragments of dark-field analysis of a columnar grain structure. As examples of columnar grains, arrows *1* and *2* in Fig. 2a indicate the regions the orientation of which is unfavorable for growth. These regions are grains, since the extinction contour corresponding to an operating reflection is not excited in them in the angle of inclination range at least 8° and the neighboring regions are in a reflecting position. The length of these regions reaches ≈200 nm at a width of 30–50 nm.

The width of the columnar grains corresponding to the texture component changes from several tens to 300–400 nm. (Examples of grains of various sizes are indicated by the arrow in Fig. 2b). The grain sizes change (the widths of some grains increase and those of others decrease) with the coating thickness, which indicates different growth abilities of crystals of different orientations (with a wide spectrum of azimuthal misorientations) within the in-plane texture. The columnar grains of the give sizes are divided into subgrains 200–250 nm in length and 25–40 nm in transverse size, which are elongated in the growth direc-

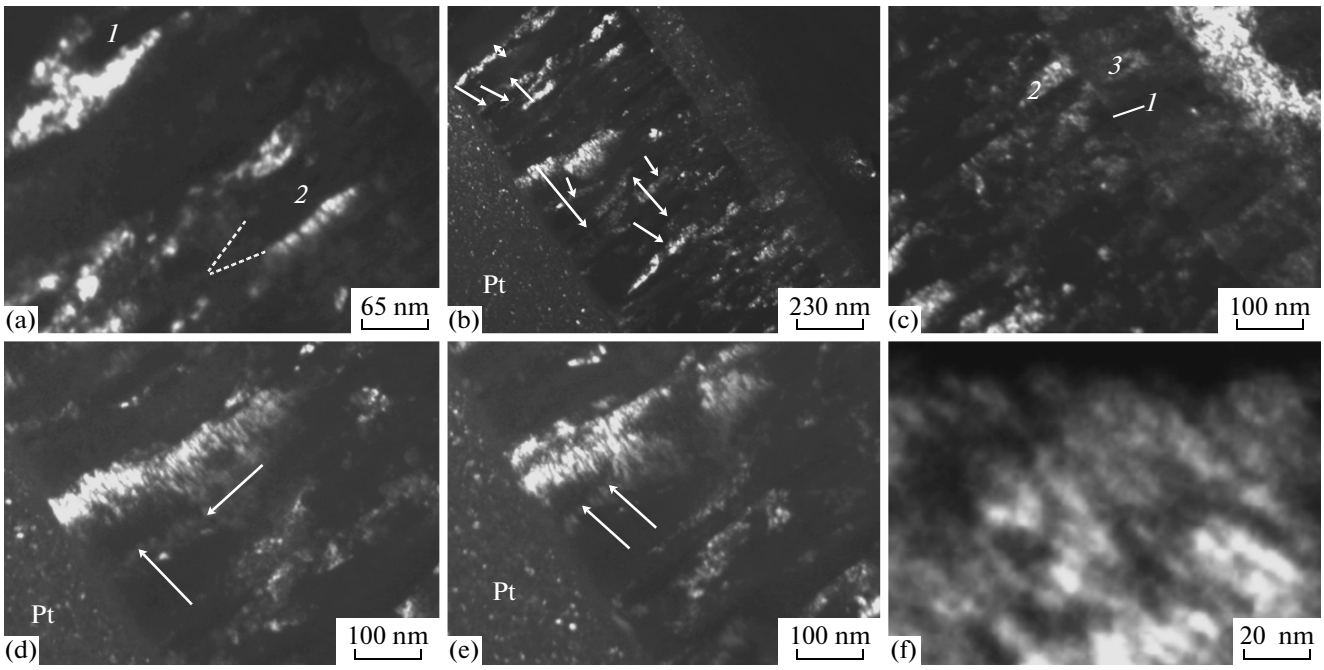

Fig. 2. Dark-field images of the structure of a titanium nitride–based coating (see text).

tion, by longitudinal low-angle boundaries (one-sided arrows in Fig. 2b).

According to a dark-field image of the structure of the interface between the coating and the TiN–α-Ti gradient layer, the orientations of the reflecting planes of the coating (arrow 2) and the sublayer (arrow 3) are close to each other (Fig. 2c). This fact is likely to evidence possible epitaxial nucleation of coating crystals on TiN crystals in the nitrided sublayer. Moreover, a developed columnar subgrain structure with misorientations of several degrees is observed near the coating surface. This means that the misorientations of the adjacent volumes change along subgrain boundaries and increase along the growth direction. One of these boundaries is shown in Figs. 2d and 2e (indicated by arrows). It follows from a comparison of these images that, at an inclination of 2.5°, the contour in the upper crystal with respect to the boundary shifts ≈90 nm to the left and the crystal below the boundary is in a reflecting position over the entire angle of inclination range. Therefore, a misorientation vector gradient of ≈25 deg/μm takes place along the boundary. A structural model of the grain volume that corresponds to the misorientation vector gradient can be represented by a state with an excess density of dislocations of the same sense, which determine the elastoplastic bending–torsion of the crystal lattice on either side of the boundary. In particular, the density of such dislocations estimated from the relation $\rho_{\pm} = (d\varphi/dr)/b$ gives $\approx 1.5 \times 10^{11}$ cm^{-2}; here, $d\varphi/dr$ is the misorientation vector gradient and b is the Burgers vector of dislocations.

The defect structure of the coating is represented by a dislocation network formed by long (100–120 nm) dislocations or dislocation tangles with transverse dislocations, which intersect an entire subgrain, and the distance between them is 6–8 and 5 nm, respectively. Thus, the dislocation density in the network reaches $\approx 2 \times 10^{12}$ cm^{-2}. This value is an order of magnitude higher than the excess dislocation density.

The homogeneity of the dislocation structure in a subgrain should be noted. In this case, the local bending–torsion of the crystal lattice can significantly exceed the misorientation vector gradient along a boundary (25 deg/μm) and reach 80–90 and 70 deg/μm for the crystallographic planes that are perpendicular and parallel to the growth direction, respectively.

3.2. Micro- and Substructure of the Coating in Indentation Zones

When processing load–indentation depth curves, we were able to find the hardness (≈22 GPa), Young's modulus (≈240 GPa), fracture toughness (≈1.15 MPa m$^{0.5}$), and the specific work of adhesion coating separation (≈800 J/m^2) [25].

The results of electron-microscopic investigations of the coating structure in the indentation zones that formed at a load up to 200 mN demonstrate that the coating retains its integrity at a distance of 1–1.5 μm from the indentation vortex. Cracks, which are similar to the crack shown in Fig. 3a, are observed at the periphery of the indentation. Sometimes, they reach

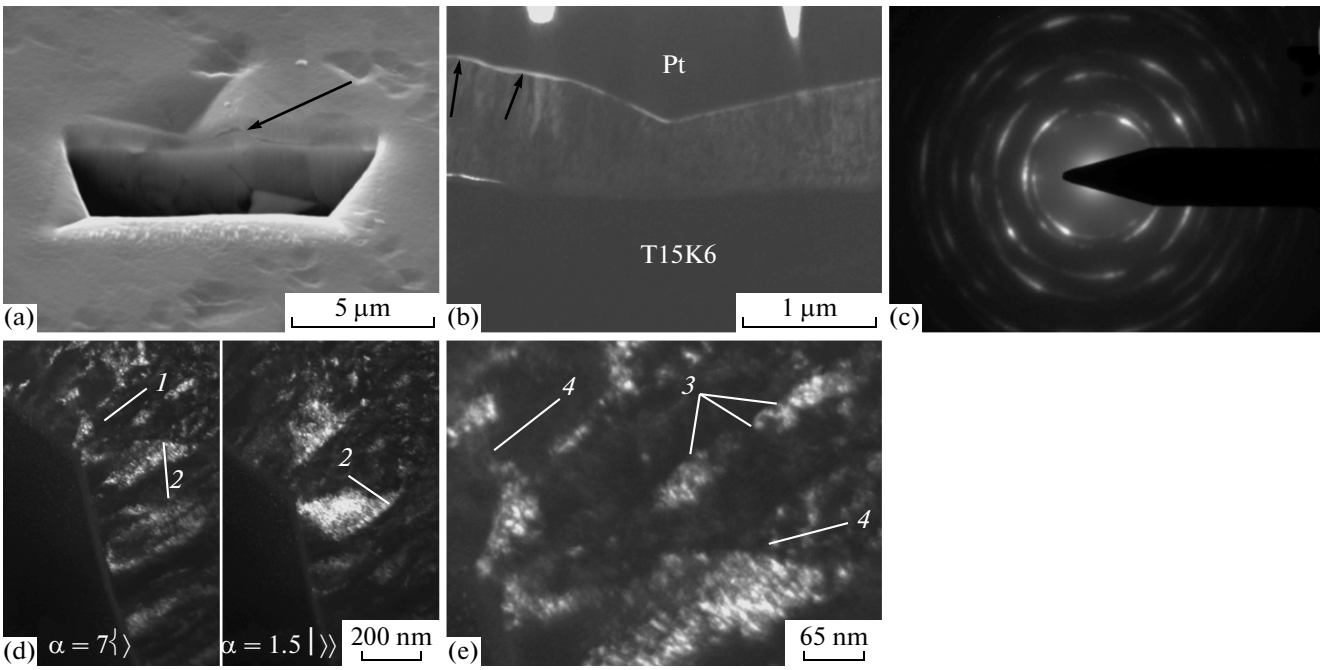

Fig. 3. Structure of titanium nitride–based coating in the cross section of the indentation zone: (a) scanning electron microscopy, (b)–(e) transmission electron microscopy, (b) bright-field image, (c) electron diffraction pattern, and (d), (e) dark-field image.

the α-Ti sublayer or grow into it from substrate asperities, and the substrate can undergo brittle fracture along grain boundaries in the indentation zone.

It should be noted that the coating thickness decreased during indentation by ≈25%, from ≈0.85 to 0.64 μm in the indentation zone (Fig. 3b). No deformation (flexure) of the substrate under the indenter is observed at an indentation depth up to 700–750 nm. However, the edges of some indentation faces have an irregular shape and the asperity height can reach ≈60 nm (indicated by arrows in Fig. 3b). This can be related to the extrusion of the material from the indenter, since relief asperities associated with growth are observed on the coating surface.

The lattice parameter calculated from electron diffraction patterns in the indentation zone is $a = 0.4165 \pm 0.001$ nm, which coincides with the lattice parameter in the cross section in the undeformed state ($a = 0.418 \pm 0.00$ nm) within the limits of experimental error (Fig. 3c). However, the reflection density and the azimuthal scattering of the quasi-ring reflections taken from regions of the same size (≈300 nm) are severalfold larger for the structure in the indentation zone. This finding indicates an increase in the density of low-angle boundaries and the change of a lattice orientation in individual grains. Here, some regions of quasi-ring segments are continuous, which points to a small (at most 1°) or a quasi-continuous change in the azimuthal component of the orientation of reflecting planes.

An analysis of the dark-field image of the coating structure under the indenter vortex shown in Fig. 3d allowed us to find the following. First, one crystallographic orientation (angle of sample inclination of 7°) exist in an indentation region 400 nm in size. A grain ≈90 nm in diameter of a columnar morphology is detected at a distance of ≈100 nm under an indentation (Fig. 3d, arrow 1). Such specific features of growth, i.e., its completion at the coating surface, were not detected in the state after deposition. Second, the shape of the boundaries of columnar grains changes in some zones: they become curved (Fig. 3d, arrows 2). This change can cover significant coating volume, sometimes from the coating surface to the nitrided sublayer. The curved boundaries have a faceted structure, i.e., numerous steps along the normal to the growth direction (Fig. 3e, arrows 3). Third, as compared to the initial state, the density of transverse low-angle boundaries, which essentially form new subgrains, increases in the indentation zone. This density reaches ≈8.5 deg/μm in the indentation vortex zone, which is approximately twice as large as that in the undeformed sample. Some grains have a length of 100–150 nm and their misorientations reach 5° (Fig. 3e, arrows 4).

The defect structure in the indentation zone is analogous to that detected in the as-deposited state: it is represented by a dislocation network with a dislocation density of $\approx 2 \times 10^{12}$ cm^{-2} (Figs. 4a, 4b). No unidirectional motion of an extinction contour across subgrains was detected. However, quasi-continuous motion of an extinction contour and similar lattice bending–torsion can be determined in some regions at an angle of sample inclination of 0.5°. For example, in the region indicated by arrow 2 in Figs. 4a and 4b, the

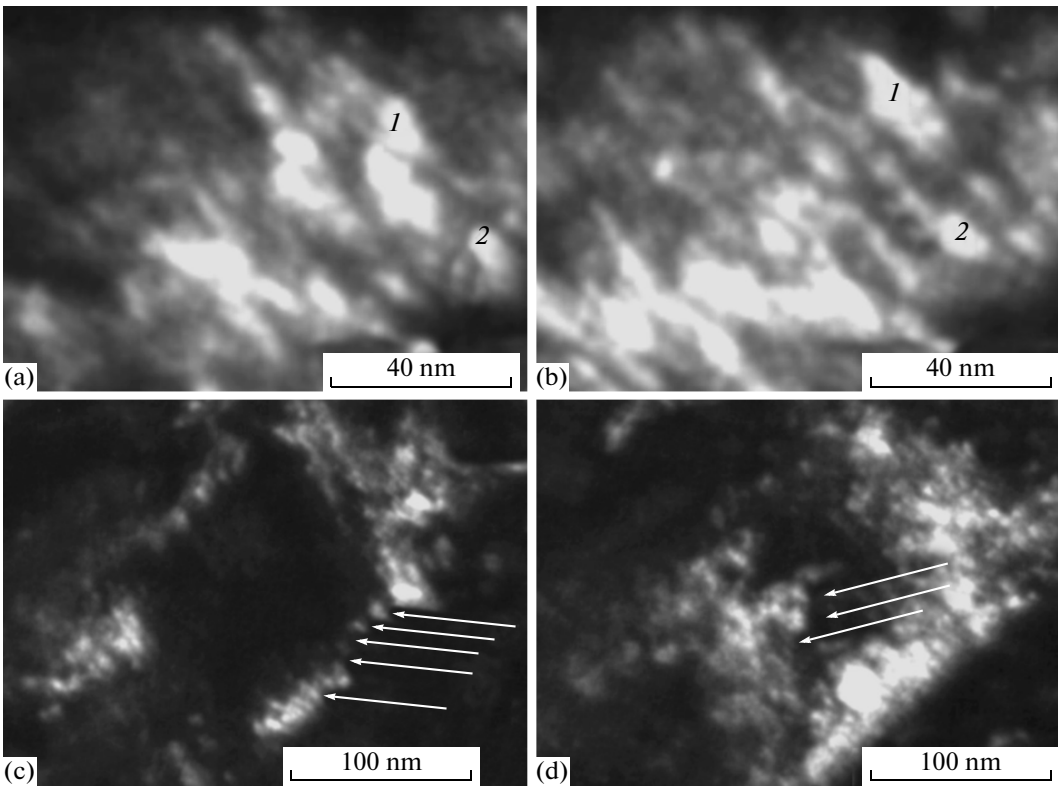

Fig. 4. Dark-field images of a titanium nitride–based coating at the indentation vortex: (a), (b) motion of extinction contours and (c), (d) dislocation structure (see text).

extinction contour shifts ≈7 nm to the left and up when the angle of inclination changes from 7.5° (Fig. 4a) to 7° (Fig. 4b). This shift is caused by the bending of the crystallographic planes that are perpendicular to the electron beam, and this bending–torsion is ≈70°/μm [22, 23]. A similar analysis of the contour motion in the region indicated by arrow 1 in Figs. 4a and 4b gives a bending–torsion of ≈50 deg/μm.

The shifts of an extinction contour at such angles of inclination are on the order of the sell size in a network dislocation structure. Therefore, the reorientation of the material in the regions under study can be discrete and related to the structural defects that form cells. As noted above, the network dislocation structure is formed by long parallel dislocations, which move through an entire subgrain and weakly change their direction. In some cases (e.g., those indicated by the arrows in Figs. 4c, 4d), the material volume in a certain length of these dislocations is misoriented with respect to the adjacent volumes so that a structure with a periodic change in the orientation forms. Therefore, we can assume that these dislocations can be dislocation dipoles.

4. DISCUSSION OF RESULTS

As noted above, the coating formed by magnetron sputtering has an in-plane {110} texture at a wide range of azimuthal orientations on the growth surface. It is known [8] that such a texture forms from an axial texture at a tilted location of a substrate with respect to plasma streams. Therefore, this azimuthal scattering of reflections reflects insufficient development of an in-plane texture because of, first, a relatively small coating thickness and, second, a decrease in the time of tiled deposition, since certain part of deposition occurs during perpendicular incidence of a gas–plasma flow on the substrate plane because of short substrate fixation in the corresponding position.

One of the mechanisms of texture formation in the coating upon the completion of competitive columnar grain growth is surface diffusion of adsorbed atoms from grains to grains, which results in a change in the grain size [8]. Therefore, it was interesting to estimate the surface diffusion coefficient from the following data. The columnar grain 2 width decreases uniformly from 38 nm to zero in a length of 50 nm (Fig. 2a, dashed line), which corresponds to a growth time of ≈500 s (Fig. 2). In other words, the grain diameter decreases by about 0.15 nm in 2 s. We put 0.15 nm equal to the mean diffusion length $(2D_{sur} \times 2\ s)^{0.5}$ expressed through the surface diffusion coefficient and find that this coefficient is 5.6×10^{-21} m^2/s.

According to the results of studying the bending–torsion of the coating lattice in the region of the coating–substrate interface, we find that the orientations of the reflecting planes in the coating and the TiN layer

formed by ion nitriding of α-Ti are close to each other. This crystal-geometric relation is likely to favor a similar orientation of crystallographic coating nucleation centers along a significant (several hundred nanometers) distance along the interface between the nitrided sublayer and the coating with predominant low-angle boundaries. The density of these boundaries is an order of magnitude higher than the density of high-angle boundaries. One of the horizontal components of the misorientation vector can reach several degrees in the surface layer with allowance for the detected increase in the misorientation between low-angle boundaries (Figs. 2d, 2e).[1]

The detected increase in the misorientation angles at subgrain boundaries can be the manifestation of growth stress relaxation, which results in a change in the structure of low-angle boundaries when they absorb lattice dislocations, and/or can reflect the increase in the elastoplastic lattice bending–torsion in the subgrain volume when the density of dislocations of the same sense increases in subgrains. This increase in the defect density with the coating thickness forms a gradient composite material with a high surface strength. Therefore, all cracks detected in the cross sections of indentations are likely to nucleate and propagate to a distance of at least half the coating thickness from the coating surface.

All cracks are detected at the contact interface where the loaded surface bends. It is known [15, 28] that a complex state of stress forms in these regions both during loading and after unloading. The state of stress across an indentation changes along both the coating thickness and in the cross section relative to the indentation direction, and this state is characterized by the existence of shear and compressive (under indentation) or tensile (at a certain distance from an indentation) stresses. A combination of these stresses can lead to the formation of mode I and II cracks. In addition, the tensile stresses that operate at an angle of 45° to the normal to the surface in the bending zone at the edge of the indenter–coating contact can result in crack opening in the sublayer, which undergoes compression and shear in the transverse direction [28]. Under these conditions, cracks are known to form along a compression direction, i.e., in the transverse direction [29].

In the case of comparable coating and substrate hardnesses, the coating mainly deforms at an almost unchanged substrate surface shape under an indentation. The absence of bending the substrate should substantially decrease the transverse tensile stresses at the coating–substrate interface and in the periphery of the indentation. Moreover, a finite element simulation of the state of stress in the coating–substrate system showed that the peak tensile stresses related to the shear stresses decrease as the strength properties of the substrate increase (in particular, upon the substitution of high-speed steel for aluminum) [28]. This behavior should decrease the probability of cracking along columnar boundaries. Note that we did not detect such cracks in this work. Moreover, in contrast to [16, 17, 21], the increase in the relative shear stresses at the coating–substrate interface does not relax with the formation of steps in it when individual columnar grains glide. Along with the decrease in the coating thickness under an indentation, these facts indicate plastic deformation of the coating.

Note that the increase in the azimuthal misorientations under an indentation detected in the cross section points to an increase in the bending of reflecting planes in the coating growth direction. This behavior corresponds to a macroscopic character of the coating deformation, namely, nonuniform compression along the indentation axis and shear in the transverse direction. On a microstructure level, deformation changes the characteristics of the interface–high- and low-angle boundaries ensemble. In this case, the characteristic boundary shape (bending toward the growth direction) and the increase in the density of transverse low-angle boundaries and steps at boundaries also correlate with the detected macroscopic character of the state of stress.

It is interesting that extended columnar structure boundaries are absent in the indentation zone under the indenter vortex, where the compressive stresses are maximal. This fact is likely to indicate breaking of such boundaries under the vortex or their migration under stresses in the directions that are transverse to the indenter axis. Obviously, the formation of new low-angle boundaries is a relaxation process, which is caused by high stresses and the density of excess dislocations of the same sense under the indenter.

CONCLUSIONS

(1) The conditions of the deposition of titanium nitride–based coatings determine the competitive growth of columnar grains up to complete disappearance of some of them as a coating grows.

(2) The structure of columnar coatings is formed by submicron columnar grains, which are divided into subgrains 30–50 nm in size by low-angle boundaries with a high scalar dislocation density (up to 2×10^{12} cm^{-2}) that are extended in the growth direction in a network intrasubgrain structure at a significantly lower (by an order of magnitude) excess density of dislocations of the same sense.

(3) A crystallographic relation was found between the formed ion–plasma nitrided α-Ti TiN sublayer and the adjacent coating crystals.

(4) Inclined bent cracks were detected at the periphery of the indenter–coating contact when slip is suppressed (because of high substrate hardness), and

[1] Although the possibility of changing the orientation columnar crystals during growth was noted earlier [26, 27], we do not know analogs of the quantitative estimates presented in this work. Such estimates can be important to analyze the strength characteristics of the material and to predict the microhardness behavior of the material as a whole.

cracking along the boundaries of columnar crystals was observed.

(5) The significant decrease in the coating thickness under the indenter vortex at an unchanged substrate shape indicates plastic deformation of the coating. On a microscopic level, this deformation manifests itself in an increase in the density, the misorientation, and the nonequilibrium of the interface.

ACKNOWLEDGMENTS

This work was supported by the Russian Foundation for Basic Research (project no. 13-08-00502) and the Materials Science Center of Joint Use of Tomsk State University.

REFERENCES

1. P. J. Martin, A. Bendavid, J. M. Cairney, and M. Hofman, "Nanocomposite Ti–Si–N, Zr–Si–N, Ti–Al–Si–N, Ti–Al–V–Si–N thin films coatings deposited by vacuum arc deposition," Surf. Coat. Technol. **200**, 2228– 2235 (2005).
2. P. Zeman, R. Čerstvy, P. H. Mayrhofer, C. Mitterer, and J. Musil, "Structure and properties of hard and superhard Zr–Cu–N nanocomposite coatings," Mat. Sci. Eng. A **289**, 189–197 (2000).
3. J. Šůna, J. Musil, V. Ondok, and J. R. Han, "Enhanced hardness in sputtered Zr–Ni–N films," Surf. Coat. Technol. **200**, 6293–6297 (2006).
4. M. Audronis, P. J. Kelly, A. Leyland, and A. Matthews, "The effect of pulsed magnetron sputtering on the structure and mechanical properties of CrB2 coatings," Surf. Coat. Technol. **201**, 3970–3976 (2006).
5. J. Neidhardt, Z. Czigany, B. Sarrtory, et al., "Nanocomposite Ti–B–N coatings, synthesized by reactive arc evaporation," Acta Materialia **54**, 4193–4200 (2006).
6. F. Medjani, R. Sanjines, G. Allidi, and A. Karimi, "Effect of substrate temperature and bias voltage on the crystallite orientation in RF magnetron sputtered AlN thin films," Thin Solid Films **515**, 260–265 (2006).
7. C. V. Falub, A. Karimi, M. Ante, and W. Kalls, "Interdependence between stress and texture in arc-evaporated Ti–Al–N thin films," Surf. Coat. Technol. **201**, 5891–5898 (2007).
8. S. Mahieu, P. Ghekiere, D. Depla, and R. De Gryse, "Biaxial alignment in sputter deposited thin films. Review," Thin Solid Films **515**, 1229–1249 (2006).
9. C. H. Ma, J. H. Huang, and H. Chen, "Texture evolution of transition nitride-metal thin films by ion beam assisted deposition," Thin Solid Films **446**, 184–193 (2004).
10. P. H. Mayrhofer, C. Mitterer, L. Hultman, and H. Clemens, "Microstructural design of hard coatings," Prog. Mater. Sci. **51**, 1032–1114 (2006).
11. R. Daniel, K. J. Martischitz, J. Keckes, and C. Mitterer, "The origin of stresses in magnetron-sputtered thin-films with zone T structures," Acta Materialia **58**, 2621–2633 (2010).
12. D. Rafaja, C. Wustefeld, M. Dopita, et al., "Formation of defect structures in hard nanocomposites," Surf. Coat. Technol. **203**, 572–578 (2008).
13. N. J. M. Carvalho, E. Zoesbergen, B. J. Kooi, and J. T. M. De Hosson, "Stress analysis and microstructure of PVD monolayer TiN and multilayer Ti/(Ti, Al)N coatings," Thin Solid Films **429**, 179–189 (2003).
14. G. Jaeger, I. Endler, M. Heilmaier, K. Bartsch, and A. Leonhardt, "A new method of determining strength and fracture toughness of hard coatings," Thin Solid Films **377–378**, 382–388 (2000).
15. V. Jayaram, S. Bhowmick, Z. H. Xie, et al., "Contact deformation of TiN coatings on metallic substrates," Mat. Sci. Eng. A **423**, 8–13 (2006).
16. L. W. Ma, J. M. Cairney, M. Hoffman, and P. R. Munroe, "Deformation mechanisms operating during nanoindentation of TiN coatings on steel substrates," Surf. Coat. Technol. **192**, 11–18 (2005).
17. N. J. M. Carvalho and J. T. M. De Hosson, "Deformation mechanisms in TiN/(Ti, Al)N multilayers under depth-sensing indentation," Acta Materiallia **54**, 1857–1862 (2006).
18. J. M. Molina-Aldarequia, S. J. Lloyd, M. Oden, et al., "Deformation structures under indentation in TiN/NbN single-crystal multilayers deposited by magnetron sputtering at differing bombarding ion energies," Phil. Mag. A **82**, 1983–1992 (2002).
19. N. Verma, S. Cadambi, V. Jayaram, and S. K. Biswas, "Micromechanisms of damage nucleation during contact deformation of columnar multilayer nitride coatings," Acta Materialia **60**, 3063–3073 (2012).
20. Z. H. Xie, M. Hoffman, P. Munroe, A. Bendavid, and P. J. Martin, "Deformation mechanisms of TiN multilayer coatings alternated by ductile or stiff interlayers," Acta Materialia **56**, 852–861 (2008).
21. J. M. Cairney, M. Hoffman, P. Munroe, P. J. Martin, and A. Bendavid, "Deformation and fracture of Ti–Si–N nanocomposite films," Thin Solid Films **479**, 193–200 (2005).
22. A. N. Tyumentsev, A. D. Korotaev, Yu. P. Pinzhin, et al., "Defect microstructure in submicrocrystalline titanium nitride crystals," Izv. Vyssh. Uchebn. Zaved., Fiz., No. 7, 3–12 (1998).
23. A. D. Korotaev, D. P. Borisov, V. Yu. Moshkov, et al., "Nanocomposite and nanostructured superhard Ti–Si–B–N coatings," Perspektivnye Materialy, No. 2, 55–67 (2009).
24. *Nanostructured Coatings*, Ed. by A. Cavaleiro and J. T. H. De Hosson (Springer, New York, 2006).
25. S. V. Ovchinnikov, A. D. Korotaev, Yu. P. Pinzhin, and S. V. Popov, "Examination of the features of the structural states of alloyed titanium-nitride-based in strain and fracture bands by nanoindentation and scratch testing," Izv. Vyssh. Uchebn. Zaved., Fiz. **12** (2), 238–242 (2012).
26. A. D. Korotaev, V. Yu. Moshkov, S. V. Ovchinnikov, et al., "Nanostructured and nanocomposite superhard coatings," Fizicheskaya Mezomekhanika **8** (5), 103–116 (2005).
27. F. S. Shieu, L. H. Cheng, Y. C. Sung, J. H. Huang, and G. P. Yu, "Microstructure and coating properties of ion plated TiN on type 304 stainless steel," Thin Solid Films **334**, 125–132 (1998).
28. M. T. Tilbrook, D. J. Paton, Z. Xie, and M. Hoffman, "Microstructural effect of indentation failure mechanisms in TiN coatings: finite element simulations," Acta Materialia **55**, 2489–2501 (2007).
29. R. R. Balokhonov and V. A. Romanova, "The effect of the irregular interface geometry in deformation and fracture of a steel substrate–boride coating composite," Int. J. Plasticity **25**, 2025–2044 (2009).

Translated by K. Shakhlevich

SPELL: 1. ok